

Article

A Deformation Analysis Method for Sluice Structure Based on Panel Data

Zekai Ma^{1,2}, Benxing Lou^{1,2,3,*}, Zhenzhong Shen^{1,2}, Fuheng Ma^{3,*}, Xiang Luo^{1,2,3}, Wei Ye³, Xing Li³ 
and Dongze Li^{1,2}

¹ The National Key Laboratory of Water Disaster Prevention, Hohai University, No. 1 Xikang Road, Nanjing 210024, China

² College of Water Conservancy and Hydropower Engineering, Hohai University, No. 1 Xikang Road, Nanjing 210024, China

³ Department of Dam Safety and Management, Nanjing Hydraulic Research Institute, No. 223 Guangzhou Road, Nanjing 210098, China

* Correspondence: bxlou@hhu.edu.cn (B.L.); fhma_nhri@163.com (F.M.)

Abstract: Deformation, as the most intuitive index, can reflect the operation status of hydraulic structures comprehensively, and reasonable analysis of deformation behavior has important guiding significance for structural long-term service. Currently, the health evaluation of dam deformation behavior has attracted widespread attention and extensive research from scholars due to its great importance. However, given that the sluice is a low-head hydraulic structure, the consequences of its failure are easily overlooked without sufficient attention. While the influencing factors of the sluice's deformation are almost identical to those of a concrete dam, nonuniform deformation is the key issue in the sluice's case because of the uneven property of the external load and soil foundation, and referencing the traditional deformation statistical model of a concrete dam cannot directly represent the nonuniform deformation behavior of a sluice. In this paper, we assume that the deformation at various positions of the sluice consist of both overall and individual effects, where overall effect values describe the deformation response trend of the sluice structure under external loads, and individual effect values represent the degree to which the deformation of a single point deviates from the overall deformation. Then, the random coefficient model of panel data is introduced into the analysis of sluice deformation to handle the unobservable overall and individual effects. Furthermore, the maximum entropy principle is applied, both to approximate the probability distribution function of individual effect extreme values and to determine the early warning indicators, completing the assessment and analysis of the nonuniform deformation state. Finally, taking a project as an example, we show that the method proposed can effectively identify the overall deformation trend of the sluice and the deviation degree of each measuring point from the overall deformation, which provides a novel approach for sluice deformation behavior research.

Keywords: sluice; nonuniform deformation; random coefficient model; individual effect values; maximum entropy principle



Citation: Ma, Z.; Lou, B.; Shen, Z.; Ma, F.; Luo, X.; Ye, W.; Li, X.; Li, D. A Deformation Analysis Method for Sluice Structure Based on Panel Data. *Water* **2024**, *16*, 1287. <https://doi.org/10.3390/w16091287>

Academic Editor: Helena M. Ramos

Received: 28 March 2024

Revised: 19 April 2024

Accepted: 26 April 2024

Published: 30 April 2024



Copyright: © 2024 by the authors. Licensee MDPI, Basel, Switzerland. This article is an open access article distributed under the terms and conditions of the Creative Commons Attribution (CC BY) license (<https://creativecommons.org/licenses/by/4.0/>).

1. Introduction

The sluice is a common hydraulic structure that plays a very important role in controlling flooding, reducing disaster, optimizing water resource allocation, and protecting the ecological environment [1,2]. During service periods, the sluice's safety will be threatened by multiple risks such as external loads and emergencies, and it is necessary to grasp the work state of the project through structural safety evaluation. Deformation, as the most intuitive index, can comprehensively reflect the operation status of the sluice [3], and therefore, reasonable analysis and evaluation of sluice deformation behavior have important guiding significance for its long-term service [4].

Structural deformation is an important research topic in safety evaluation areas of hydraulic engineering at all times. Much research to date has focused on the analysis methods of dam deformation behavior [5,6], in which the statistical model is most commonly used to establish the relationship between deformation and influencing factors, including water level, temperature, and concrete creep [7–9]. In order to improve the accuracy and robustness of the statistical model, scholars introduced some artificial intelligence methods [10,11], including artificial neural networks [12,13], support vector machines [14,15], and deep learning model [16,17], into the analysis of dam deformation. However, because it is a low-head hydraulic structure, the safety of the sluice is easily overlooked without adequate attention [18]. Although the deformation analysis method of a concrete dam can be referenced for the sluice, there exist some significant differences in their deformation characteristics. For a concrete dam, the deformation of a certain measuring point or dam section is the focus of attention because of the high water pressure. For the sluice, the nonuniform deformation between different measuring points should attract special attention, owing to the uneven feature of ground properties and load distribution [19]. Especially before the deformation develops stably, the sluice structure is likely to incur nonuniform deformation, even leading to serious accidents such as waterstop failure, buildings tilting, and concrete slab fracture [20].

In the actual project, the deformations of measuring points in different parts of the sluice are different due to the nonuniformity of external loads and soft soil foundations, but the overall deformation trend is still similar because of the similar service environment. Hence, the deformation of a sluice could be divided into two parts: overall effect values and individual effect values, where overall effect values describe the deformation response trend of the sluice structure under external loads, and individual effect values represent the deviation degree between the deformation of a single point and the overall deformation. The panel data theory was first put forward by Mundlak in 1961, and has been introduced widely into the fields of econometrics, sociology, and market research. Several studies on dam deformation have been published using panel data theory, which paid greatest attention to the spatial correlation as well as the determination of abnormal areas for dam deformation. For instance, Shi et al. [21] proposed a variable intercept panel model based on deformation zoning of ultra-high arch dams, and subsequently, two panel models were established to distinguish the fixed and random modes of special effects of dam deformation. Shao et al. [22] proposed a random coefficient model using panel data theory, which can solve the serious multicollinearity problem among influence factors in the traditional regression method. Zhao et al. [23] established a functional relationship between the measured values and the real-time risk probability based on the estimation of robustness of the panel model. Cui et al. [24] proposed a novel imputation model for missing concrete dam deformation data based on their evaluation of the accuracy of the panel model. In fact, one of the main uses of panel data theory is to handle the unobservable individual or overall effects [25], and we can utilize panel data theory to identify the individual effects of each measurement point, and further to evaluate the nonuniform deformation status of the sluice.

In light of the above analysis, this article introduces the panel data theory into sluice deformation analysis for identifying the overall effect values of sluice structure and the individual effect values of each measurement point. Then, the maximum entropy principle is employed to estimate the probability distribution function of individual effect extreme values, and subsequently an analysis method for the nonuniform deformation state of the sluice is developed. Finally, the deformation data of a sluice obtained through wire alignment transducer offer an example to validate the approach proposed.

2. Influencing Factors of Sluice Displacement

Referring to the statistical model of dam deformation, the influencing factors of sluice deformation δ can be divided into three parts, including water pressure component δ_H , temperature component δ_T , and aging component δ_θ , as shown in Equation (1).

$$\delta = \delta_H + \delta_T + \delta_\theta \tag{1}$$

2.1. Water Pressure Component

The sluice’s deformation under upstream and downstream water pressure consists of three parts (see Figure 1): (a) horizontal sliding deformation caused by the water pressure difference; (b) bending deformation of the structure due to movement; and (c) rotation deformation of the foundation because of water gravity difference. The horizontal displacement can be expressed as:

$$\delta_H = \delta_H^a + \delta_H^b + \delta_H^c \tag{2}$$

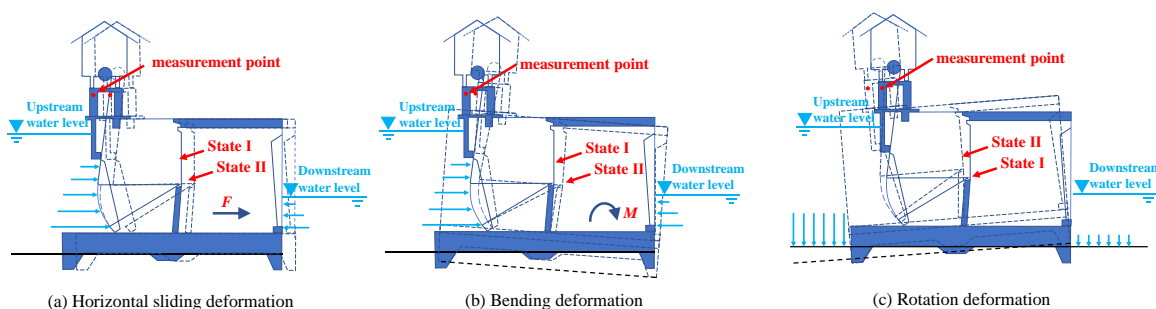


Figure 1. Schematic diagram of the water pressure component of sluice displacement.

The relationship between water pressure and water depth is quadratic, and the deformation caused by water pressure can be described as the 1–4th power of the upstream and downstream water depth, referring to the expression of the water pressure component for concrete dam deformation. Therefore, the water pressure component of sluice deformation can be expressed as:

$$\delta_H = \sum_{i=1}^4 (a_{1i}h^i + a_{2i}H^i) \tag{3}$$

where h is downstream water depth, H is upstream water depth, and a_{1i} and a_{2i} are both regression coefficients.

2.2. Temperature Component

The sluice’s deformation is also affected by the external environmental temperature. Changes in external environmental temperature will cause temperature differences in concrete structure, resulting in temperature stress and deformation. The relationship between sluice deformation and environmental temperature is shown in Figure 2, where T_i represents the average temperature of the previous i days. It can be seen that the sluice deformation directly follows environmental temperature. Therefore, the environmental temperatures within 7 days before the observation date are selected as the influencing factors, and the temperature component can be presented as:

$$\delta_T = \sum_{i=1}^m b_i T_i \tag{4}$$

where b_i is the regression coefficient.

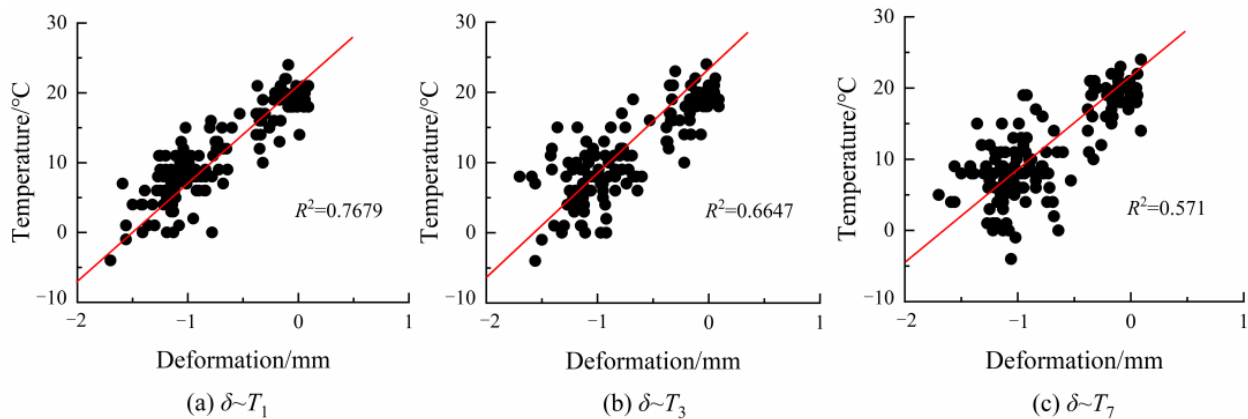


Figure 2. The correlation between deformation and temperature.

2.3. Aging Component

Due to the creep of concrete and soil foundation, the deformation of the sluice structure exhibits a certain characteristic trend, which can be depicted as:

$$\delta_\theta = c_1\theta + c_2 \ln \theta \tag{5}$$

where θ represents the difference of observation date minus start date divided by 100, and c_1 and c_2 are regression coefficients.

Thus, the statistical equations of sluice displacement can be expressed as follows:

$$\delta = \sum_{i=1}^4 (a_{1i}h^i + a_{2i}H^i) + \sum_{i=1}^7 b_iT_i + c_1\theta + c_2 \ln \theta + d \tag{6}$$

where d is a constant.

3. An Analysis Method for Sluice Displacement Behavior Based on Panel Data

3.1. Random Coefficient Statistical Model Based on Panel Data

Due to the nonuniformity of external loads and soft soil foundations, the influencing factors for each part of the sluice structure are different, which is the main reason for individual effects or uneven deformation. If we use traditional statistical models to analyze the deformation state of the sluice structure, some potential influencing factors for each part could not be included as independent variables in the model, and we would be unable to take into account the individual differences of measurement points. Therefore, in addition to considering the main factors, we should consider the unmeasurable or unknown influencing factors when modeling, so that the deformation analysis model can absorb the influence of these uncertain factors. Since traditional deformation analysis models cannot detect the individual effects caused by the hidden factors, panel data theory is introduced to identify and reveal the overall features and individual characteristics among multiple measurement points.

Panel data are two-dimensional data that include time series data and cross-sectional data [26]. Time series data reflect the observation data of a measurement point at different times, and cross-sectional data reflect the observation data of different measurement points at the same time. Firstly, we studied the variable coefficient statistical model, in which the regression coefficients of panel data do not change over time but vary cross-sectionally, formulated as follows:

$$y_{it} = \sum_{k=1}^K \beta_{ki}x_{kit} + u_{it} \tag{7}$$

where y_{it} represents the panel data form of sluice deformation data, t is the ordinal number of time data, i is the ordinal number of cross-sectional data, k is the ordinal number of

explanatory variables, x_{kit} is the explanatory variable, β_{ki} is the regression coefficient, and u_{it} is the random error.

The variable coefficient statistical model consists of both a fixed coefficient model and random coefficient model. In the fixed coefficient model, β_{ki} is considered a fixed constant and varies with individual changes. By stacking up all the deformation data, the model formula is as follows [27]:

$$\begin{bmatrix} y_1 \\ y_2 \\ \vdots \\ y_N \end{bmatrix} = \begin{bmatrix} X_1 & 0 & \cdots & 0 \\ 0 & X_2 & \cdots & 0 \\ \vdots & \vdots & \ddots & \vdots \\ 0 & 0 & \cdots & X_N \end{bmatrix} \begin{bmatrix} \beta_1 \\ \beta_2 \\ \vdots \\ \beta_N \end{bmatrix} + \begin{bmatrix} u_1 \\ u_2 \\ \vdots \\ u_N \end{bmatrix} \tag{8}$$

where $y_i = (y_{i1}, \dots, y_{iT})$ represents the time series of sluice deformation; $\beta_i = (\beta_0, \beta_1, \dots, \beta_k)'$ is the

regression coefficients to be estimated of the i -th observation point; $X_i = \begin{bmatrix} x_{11} & x_{12} & \cdots & x_{1k} \\ x_{21} & x_{22} & \cdots & x_{2k} \\ \vdots & \vdots & \ddots & \vdots \\ x_{t1} & x_{t2} & \cdots & x_{tk} \end{bmatrix}$ is

the explanatory variables matrix of the i -th observation point, and $x_{tk} = (1, H_t, H_t^2, H_t^3, H_t^4, h_t, \dots, \theta_t, \ln \theta_t)'$; and u_i is the random error of the i -th observation point.

In a fixed coefficient model, the coefficients β_i are regarded as fixed constant and independent of each other. However, because the deformation patterns change with measuring points, the parameters of β_i can be set as random variables with a common average value β . Swamy [26] proposed the following hypothesis:

$$\begin{aligned} E(\gamma_i) &= 0 \\ E(\gamma_i \gamma_j') &= \begin{cases} \Delta & (i = j) \\ 0 & (i \neq j) \end{cases} \\ E(x_{it} \gamma_j') &= 0 \\ E(\gamma_i \gamma_j') &= \begin{cases} \sigma_i^2 I_T & (i = j) \\ 0 & (i \neq j) \end{cases} \end{aligned} \tag{9}$$

Then, the random coefficients model is written with a matrix form as follows:

$$y = X\beta + \tilde{X}\gamma + u. \tag{10}$$

where $y = (y_1', \dots, y_N)'$; $X = (X_1, \dots, X_N)'$; $\tilde{X} = \begin{bmatrix} X_1 & & 0 \\ & \ddots & \\ 0 & & X_N \end{bmatrix}$; $\beta = (\beta_0, \beta_1, \dots, \beta_k)'$

is the common mean value's coefficient vector; $\gamma = (\gamma_1', \dots, \gamma_N)'$ is the deviation between individual coefficient and common average coefficient; and $u = (u_1', \dots, u_N)'$ is the random error vector.

Based on the random coefficient model, we can use $X\beta$ to represent the overall deformation for multiple measurement points, and utilize $\tilde{X}\gamma + u$ to illustrate the degree to which actual deformation of observation points deviates from overall deformation, that is, nonuniform deformation or individual effect values of observation points. For random effects models, it should be noted that the parameters obtained by least squares are not the valid parameters, and generalized least squares estimation should be selected to estimate the model coefficients.

3.2. Maximum Entropy Principle for the Probability Distribution Function of Individual Effect Extreme Values

To evaluate the health situation of nonuniform deformation for an observation point, the probability distribution function of annual or monthly individual effect extreme values should first be determined. Jaynes [28] proposed that the probability distribution with the maximum entropy should be selected while using local information to infer the global probability distribution, which is also called the maximum entropy principle.

For discrete random variables, the information entropy $H(x)$ can be expressed as:

$$H(x) = -\sum_{i=1}^n p_i \ln p_i \quad (11)$$

where p_i is the probability of variable x , and $H(x)$ is the amount of information, representing the uncertainty of random variables.

For continuous random variables, the information entropy $H(x)$ can be expressed as:

$$H(x) = -\int_R f(x) \ln f(x) dx \quad (12)$$

where $f(x)$ is the probability distribution function of variable x , and R is the integration interval.

The maximum entropy principle is used to solve the probability distribution with the maximum amount of information in light of the known sample data. Its objective function is:

$$\max H(x) = -\int_R f(x) \ln f(x) dx \quad (13)$$

The constraint conditions are:

$$\int_R f(x) dx = 1 \quad (14)$$

$$\int_R x^i f(x) dx = \mu_i \quad (15)$$

where μ_i is the i -order origin moment calculated by the known sample data. Usually, selecting a total order of 4 can describe the basic characteristics of a random variable.

To maximize the value of $H(x)$, it is necessary to continuously adjust the form of the probability distribution function $f(x)$, and the following function can be established by Lagrange multiplier method.

$$L = H(x) + (\lambda_0 + 1) \left[\int_R f(x) dx - 1 \right] + \sum_{i=1}^N \lambda_i \left[\int_R x^i f(x) dx - \mu_i \right] \quad (16)$$

Then the analytical form of the probability distribution function can be solved as follows:

$$f(x) = \exp \left(\lambda_0 + \sum_{i=1}^N \lambda_i x^i \right) \quad (17)$$

By substituting Equation (17) into Equation (14), Equation (18) can be found.

$$\lambda_0 = -\ln \left(\int_R \exp \left(\sum_{i=1}^N \lambda_i x^i \right) dx \right) \quad (18)$$

Equation (19) can be obtained by substituting Equations (17) and (18) into Equation (15).

$$\int_{\mathbb{R}} x^i f(x) dx = \int_{\mathbb{R}} x^i \exp\left(\lambda_0 + \sum_{j=1}^N \lambda_j x^j\right) dx = \frac{\int_{\mathbb{R}} x^i \exp\left(\sum_{j=1}^N \lambda_j x^j\right) dx}{\int_{\mathbb{R}} \exp\left(\sum_{j=1}^N \lambda_j x^j\right) dx} = \mu_i \quad (19)$$

For the convenience of numerical calculation, Equation (19) can be transformed into Equation (20).

$$1 - \frac{\int_{\mathbb{R}} x^i \exp\left(\sum_{j=1}^N \lambda_j x^j\right) dx}{\mu_i \int_{\mathbb{R}} \exp\left(\sum_{j=1}^N \lambda_j x^j\right) dx} = r_i \quad (20)$$

where r_i is the residual under the i -order origin moment. When solving the coefficients $\lambda_0, \lambda_1, \lambda_2, \dots, \lambda_N$, it is necessary to minimize the residual value, and the objective function can be expressed as:

$$\min r = \sum_{i=1}^N r_i^2 = \sum_{i=1}^N \left(1 - \frac{\int_{\mathbb{R}} x^i \exp\left(\sum_{j=1}^N \lambda_j x^j\right) dx}{\mu_i \int_{\mathbb{R}} \exp\left(\sum_{j=1}^N \lambda_j x^j\right) dx}\right)^2 \quad (21)$$

Therefore, the initial objective function, that is Equation (13), is converted to the form of Equation (21), and the probability distribution function of random variables can be obtained by solving Equation (21).

3.3. The Analysis Method for Nonuniform Deformation State

According to Section 3.2, the probability distribution function $f(x)$ of individual effect extreme values for each measurement point can be calculated based on the maximum entropy principle, where the annual or monthly maximum and minimum values are seen as random variables [29]. Excessive deviations from overall displacement, whether towards downstream or upstream, are detrimental to the sluice, and thus we assume that x_{α}^+ and x_{α}^- are the early warning indicators of individual effect values. When the individual effect values of the sluice exceed x_{α}^+ and x_{α}^- , the sluice will be in a warning state, and the corresponding exceeding or non-exceeding probability can be determined by Equation (22).

$$P_{\alpha} = \begin{cases} P[x > x_{\alpha}^+] = \int_{x_{\alpha}^+}^{+\infty} f(x) dx \\ P[x < x_{\alpha}^-] = \int_{-\infty}^{x_{\alpha}^-} f(x) dx \end{cases} \quad (22)$$

where P_{α} is the probability of sluice failure, which can be determined based on the importance of the sluice, generally ranging from 1% to 5%.

Based on the early warning indicators of x_{α}^+ and x_{α}^- , the following criteria can be used to determine whether the nonuniform deformation of the sluice is normal [30].

- (1) When the individual effect values meet with $x_{\alpha}^- \leq x \leq x_{\alpha}^+$, the nonuniform deformation is in a normal state;
- (2) When the individual effect values meet with $x > x_{\alpha}^+$ or $x < x_{\alpha}^-$, the nonuniform deformation is in an abnormal or warning state.

In summary, an analysis flow for nonuniform deformation behavior of the sluice is established and shown in Figure 3.

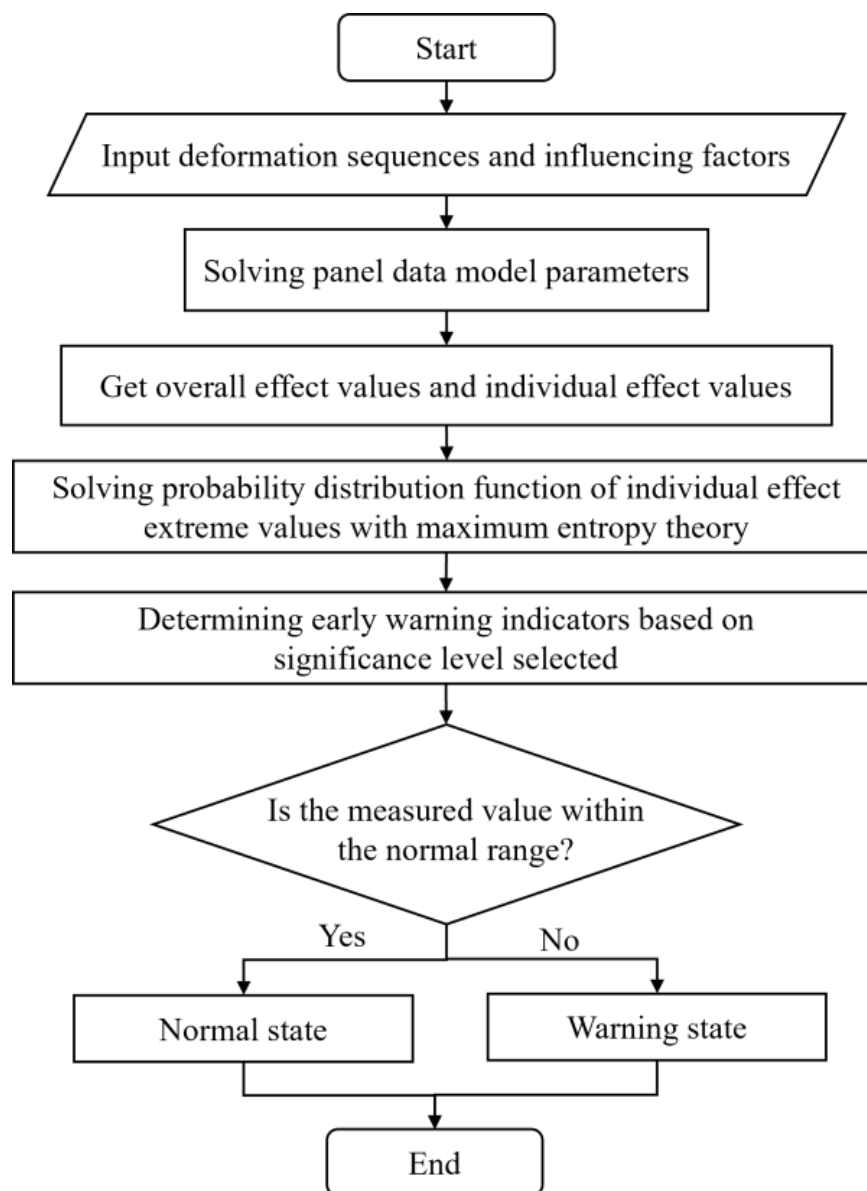
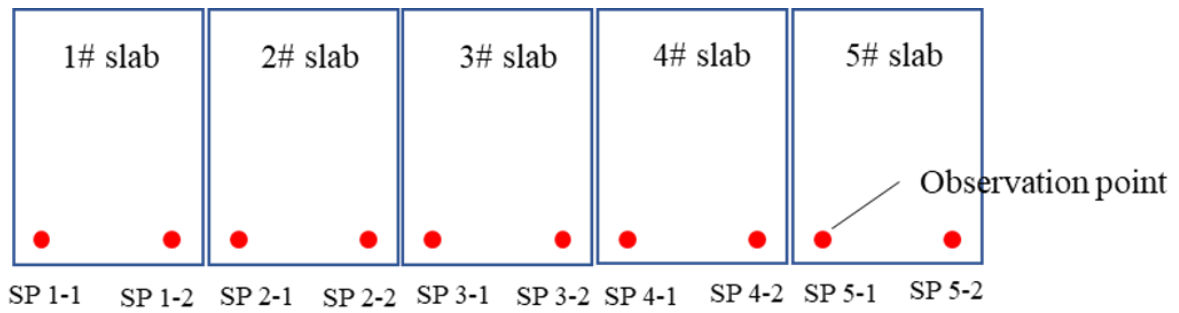


Figure 3. Flowchart of the analysis method for the sluice's deformation state based on panel data.

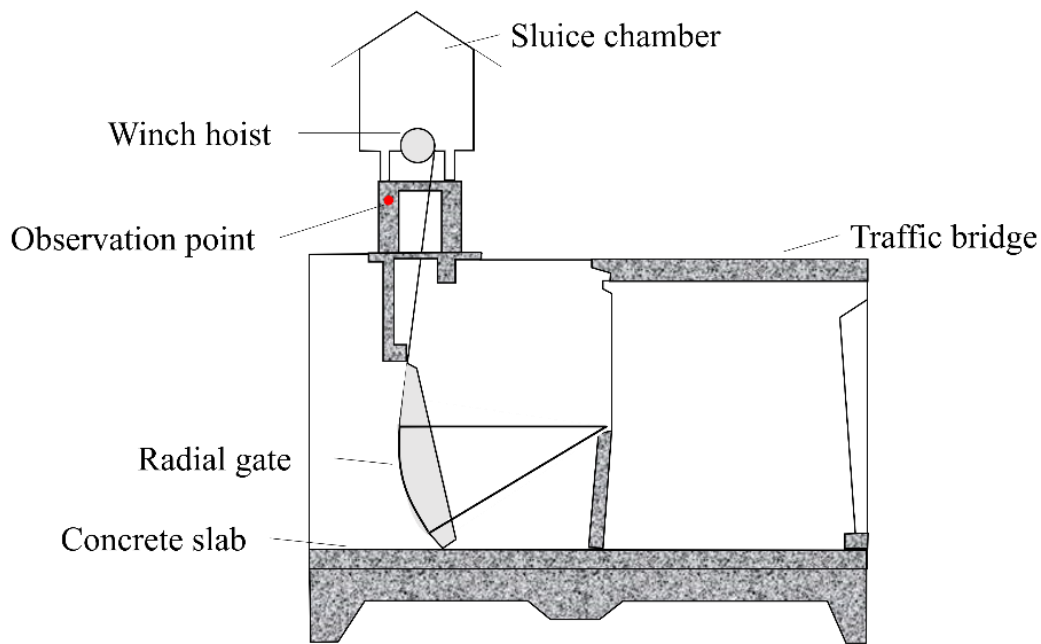
4. Case Study

4.1. General Situation

A sluice with a reinforced concrete structure is located in Jiangsu Province, China. It has 15 sluice holes with the size of $10\text{ m} \times 6.2\text{ m}$, and 5 concrete bottom slabs with the size of $33.2\text{ m} \times 18\text{ m}$. Figure 4 shows the layout of observation points for horizontal displacement set on each bottom slab, which are labeled as SP1-1, SP1-2, ..., SP5-1, and SP5-2, respectively. The deformation data of the sluice from 17 October 2022 to 5 April 2023 are presented in Figure 5, and the corresponding upstream water levels, downstream water levels, and environmental temperature are shown in Figure 6.



(a) Planar of the sluice



(b) Profile of the sluice

Figure 4. Layout of deformation measurement points for the sluice.

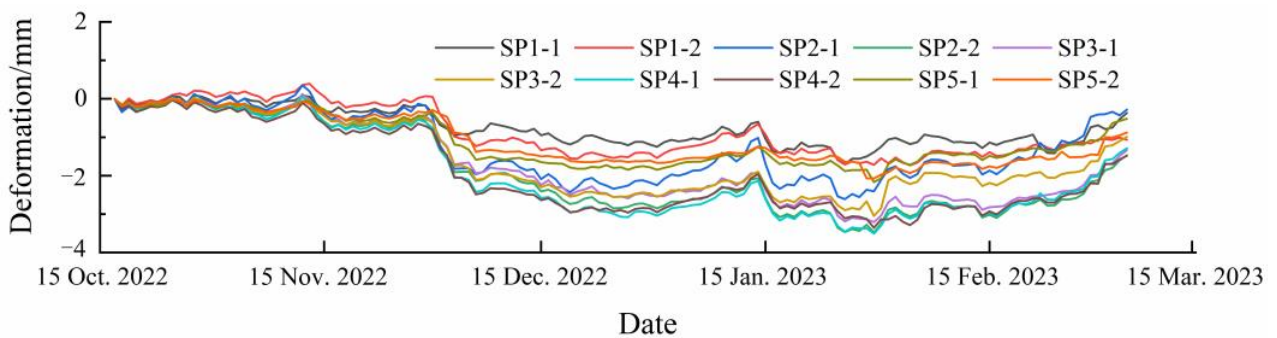


Figure 5. Deformation sequence of each measurement point of the sluice.

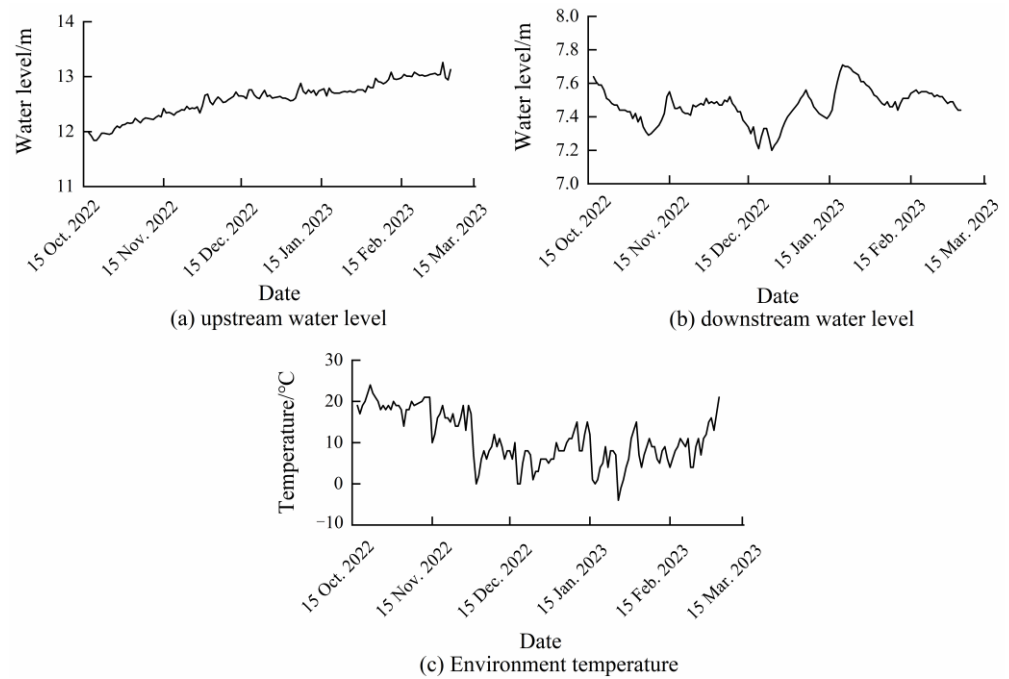


Figure 6. Environmental factor sequences.

4.2. Random Coefficient Statistical Model Based on Panel Data

4.2.1. Fitting Results

In order to verify the fitting effect of the model proposed in Section 3.1, the deformation data of the above-mentioned sluice will be taken as an example. Considering the general form of the random coefficient model, the sluice deformation statistical model can be expressed as:

$$\begin{bmatrix} y_1 \\ y_2 \\ \vdots \\ y_N \end{bmatrix} = \begin{bmatrix} X_1 \\ X_2 \\ \vdots \\ X_N \end{bmatrix} \beta + \begin{bmatrix} X_1 & 0 & \cdots & 0 \\ 0 & X_2 & \cdots & 0 \\ \vdots & \vdots & \ddots & \vdots \\ 0 & 0 & \cdots & X_N \end{bmatrix} \begin{bmatrix} \gamma_1 \\ \gamma_2 \\ \vdots \\ \gamma_N \end{bmatrix} + \begin{bmatrix} u_1 \\ u_2 \\ \vdots \\ u_N \end{bmatrix} \tag{23}$$

Firstly, each explanatory variable is normalized before modeling. Then it is possible to fit all measurement points at once based on Equation (23), and Figure 7 shows the fitted values of the random coefficient model and measured values for each measurement point. In addition, the fitting effects of the random coefficient model and stepwise regression method are compared by correlation coefficients R and standard deviation values S , as shown in Table 1. From the parameters R and S in Table 1, the results calculated by the random coefficient model are almost identical to the results calculated by the traditional stepwise regression model for each single point, with a very high fitting accuracy.

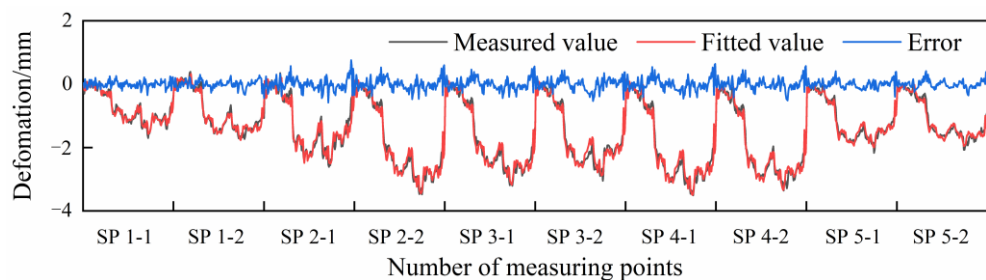


Figure 7. The fitted values of the random coefficient model and measured values of each point.

Table 1. The parameters *R* and *S* of the random coefficient model and stepwise regression method.

Random Coefficients Model						Stepwise Regression Method					
Points	<i>R</i>	<i>S</i>	Points	<i>R</i>	<i>S</i>	Points	<i>R</i>	<i>S</i>	Points	<i>R</i>	<i>S</i>
SP 1-1	0.974	0.108	SP 3-2	0.980	0.185	SP 1-1	0.974	0.108	SP 3-2	0.980	0.184
SP 1-2	0.980	0.127	SP 4-1	0.984	0.199	SP 1-2	0.981	0.127	SP 4-1	0.984	0.199
SP 2-1	0.970	0.206	SP 4-2	0.986	0.178	SP 2-1	0.970	0.206	SP 4-2	0.986	0.178
SP 2-2	0.986	0.186	SP 5-1	0.980	0.128	SP 2-2	0.986	0.186	SP 5-1	0.980	0.127
SP 3-1	0.985	0.179	SP 5-2	0.979	0.128	SP 3-1	0.985	0.179	SP 5-2	0.979	0.127

4.2.2. Identification of Overall Effect Values and Individual Effect Values

As shown by the high fitting accuracy in Section 4.2.1, it is feasible to use the random coefficient model to extract the overall effect values and individual effect values of sluice deformation. The common mean coefficients and the corresponding test statistics can be estimated by generalized least squares, as shown in Table 2. According to Table 2, the overall test result, i.e., Wald chi (12) = 209.75, and the significance test result, i.e., Prob > chi2 = 0.0, mean that using a random coefficient model to describe the sluice’s deformation is reasonable. The coefficients of h^3 , h^4 , and H^3 are all equal to 0, as they are completely collinear with other explanatory variables of water pressure components. Therefore, h^3 , h^4 , and H^3 can be removed from the model.

Table 2. Results of common mean coefficients.

Random-Coefficients Model						
R-sq: Overall = 0.986		Wald chi2(12) = 209.75			Prob > chi2 = 0.00	
var	Coefficient	Std. Err.	<i>z</i>	<i>p</i> > <i>z</i>	[95% Conf. Interval]	
<i>h</i>	−20.63	8.85	−2.33	0.020	−37.97	−3.29
h^2	1.40	0.60	2.34	0.019	0.23	2.57
h^3	0.00	(omitted)				
h^4	0.00	(omitted)				
<i>H</i>	833.66	108.05	7.72	0.000	621.89	1045.43
H^2	−50.00	6.49	−7.71	0.000	−62.71	−37.29
H^3	0.00	(omitted)				
H^4	0.053	0.007	7.70	0.000	0.04	0.07
<i>T</i> ₁	0.035	0.004	8.02	0.000	0.03	0.04
<i>T</i> ₂	0.018	0.002	7.41	0.000	0.01	0.02
<i>T</i> ₃	0.012	0.002	5.10	0.000	0.01	0.02
<i>T</i> ₄	0.021	0.002	9.04	0.000	0.02	0.03
<i>T</i> ₅	0.013	0.002	5.43	0.000	0.01	0.02
<i>T</i> ₆	0.010	0.002	4.86	0.000	0.01	0.01
<i>T</i> ₇	0.015	0.002	6.64	0.000	0.01	0.02
θ	−0.445	0.173	−2.57	0.010	−0.78	−0.11
ln θ	−0.006	0.033	−0.17	0.863	−0.07	0.06
<i>d</i>	−3.200	0.258	−12.4	0	−3.71	−2.69

The overall effect values of sluice deformation can be obtained by substituting the common mean coefficients in Table 2 into Equation (6), and the individual effect values of each measurement point can be calculated by subtracting the overall effect values from the measured value, which represents the degree of deviation from the overall deformation. Figure 8 displays the values of overall effect and individual effect for the sluice’s deformation. It can be seen that for each measuring point, the overall effect values are fixed and do not vary with the position of the measuring point, and the individual effect values are different from each other due to the nonuniformity of the external load, soil foundation, and other factors. In addition, individual effect values represent a pattern with varying measurement point positions. The individual effect values of measurement points on the 1# and 5# slabs, located on both sides of the sluice, are generally positive,

implying that individual deformation shows a tendency towards upstream relative to overall deformation, due to the constraint effect at the bank wall. The individual effect values of measurement points on the 2–4# slabs, located in the middle of the channel, are almost negative, indicating that individual deformation shows a tendency towards downstream relative to overall deformation, because the deformations of measurement points are mainly affected by the water pressure. This phenomenon is consistent with the engineering practice, proving that it is rational to distinguish the overall and individual effects of the sluice by random coefficient model.

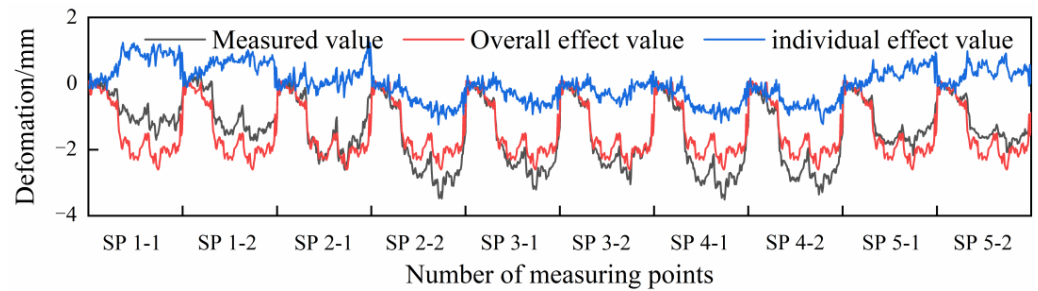


Figure 8. Overall effect values and individual effect values for each measurement point.

4.3. The Probability Distribution Function of Individual Effect Extreme Values

In Figure 8, it can be seen that the individual effect values of each measurement point are different. In order to evaluate the health status of nonuniform deformation, we firstly select the individual effect extreme values for each month, including the maximum and minimum values, and then calculate the probability distribution function of the extreme values for each measurement point separately. The coefficients $\lambda_0, \lambda_1, \lambda_2, \lambda_3,$ and λ_4 of the probability distribution function for extreme values are shown in Tables 3 and 4, and the corresponding cumulative probability curves are shown in Figure 9. It can be observed that the probability distributions are different and unique for each measurement point.

Table 3. The probability distribution function coefficients of the monthly minimum for each measurement point.

Coefficient	SP1-1	SP1-2	SP2-1	SP2-2	SP3-1	SP3-2	SP4-1	SP4-2	SP5-1	SP5-2
λ_0	-0.59	-0.22	-0.02	-4.43	-2.50	-4.73	-3.75	-10.58	0.65	0.86
λ_1	2.90	2.71	-3.35	-17.96	-8.88	-47.72	-10.45	-29.75	2.34	2.67
λ_2	2.51	0.71	-1.87	-33.56	-20.50	-149.51	-12.97	-22.07	-3.61	-17.26
λ_3	2.47	6.11	10.05	-32.01	-34.38	-199.97	-11.73	-2.24	-11.71	-30.1
λ_4	-19.89	-29.66	-8.64	-11.62	-20.49	-100.20	-5.08	0.99	-109.19	-25.23

Table 4. The probability distribution function coefficients of the monthly maximum for each measurement point.

Coefficient	SP1-1	SP1-2	SP2-1	SP2-2	SP3-1	SP3-2	SP4-1	SP4-2	SP5-1	SP5-2
λ_0	-2.89	-7.96	-0.92	-0.15	-0.11	0.35	0.04	0.11	-1.11	-1.51
λ_1	5.96	12.94	-0.05	-0.05	1.23	1.39	0.20	-1.13	2.44	7.17
λ_2	-7.10	6.02	-0.33	-4.06	-2.31	-2.02	-4.34	-7.48	-3.81	-6.85
λ_3	8.18	-2.09	2.01	-5.05	-5.95	-4.43	-5.07	-10.09	9.92	-0.05
λ_4	-3.85	-9.79	-1.28	-1.92	-3.69	-30.63	-1.79	-5.62	-7.86	0.19

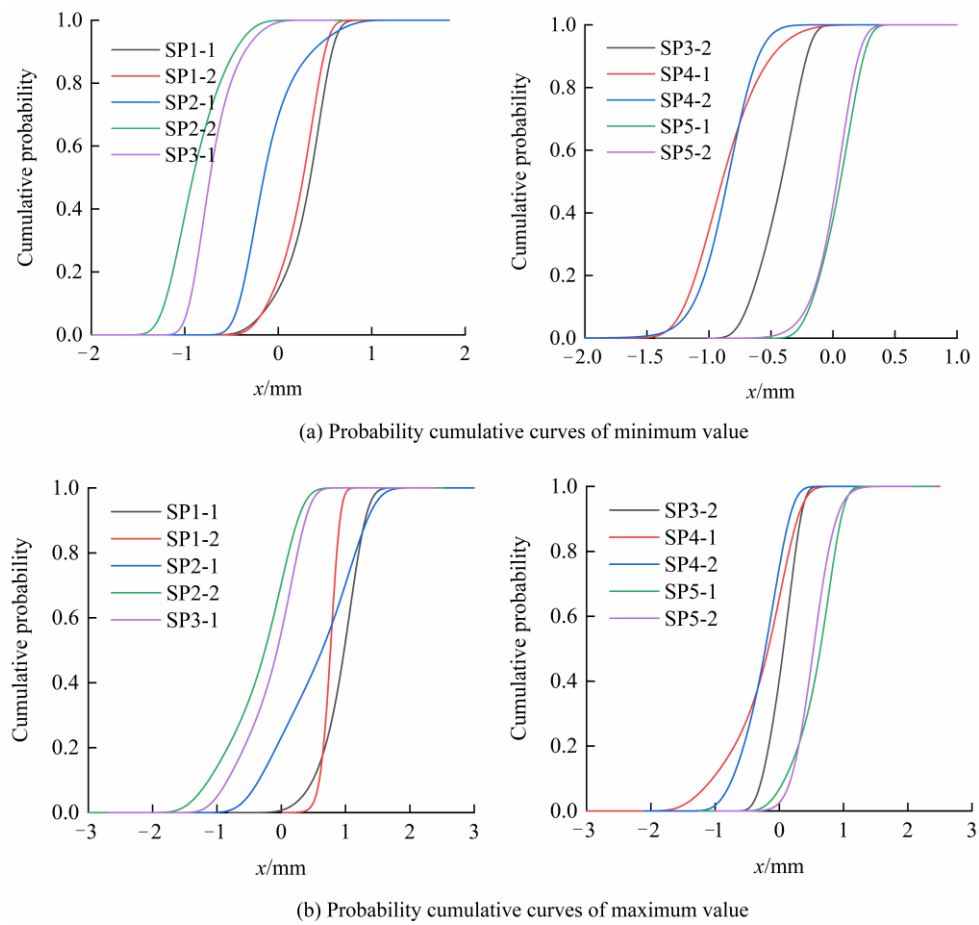


Figure 9. Probability cumulative curves for each measurement point.

4.4. Determination of Early Warning Indicators

Before determining the early warning indicators, we should first select the significance level P_α , that is, the possibility of a small-probability event occurring. In statistics, a small-probability event can be considered an almost impossible event, and if it occurs, this indicates that the deformation of the sluice is in an abnormal or warning state. The significance level is generally taken as 0.01, referring to the literature [30], and then the early warning indicators can be obtained for each measurement point, as shown in Table 5. Based on the overall effect values, we can determine the normal deformation range for each measurement point; for instance, the normal deformation ranges of points SP3-2 and SP5-2 are shown in Figure 10. When the measured values are in the normal range, it indicates that the nonuniform deformation of measurement points is in a normal state, which can assist in the judgment of the uneven deformation state of the sluice structure.

Table 5. Early warning indicator of individual effect values for each measurement point.

Measuring Point	SP1-1	SP1-2	SP2-1	SP2-2	SP3-1	SP3-2	SP4-1	SP4-2	SP5-1	SP5-2
Lower limit/mm	−0.417	−0.363	−0.580	−1.389	−1.084	−0.838	−1.399	−1.451	−0.335	−0.457
Upper limit/mm	1.504	1.020	1.657	0.521	0.599	0.479	0.536	0.368	1.141	1.190

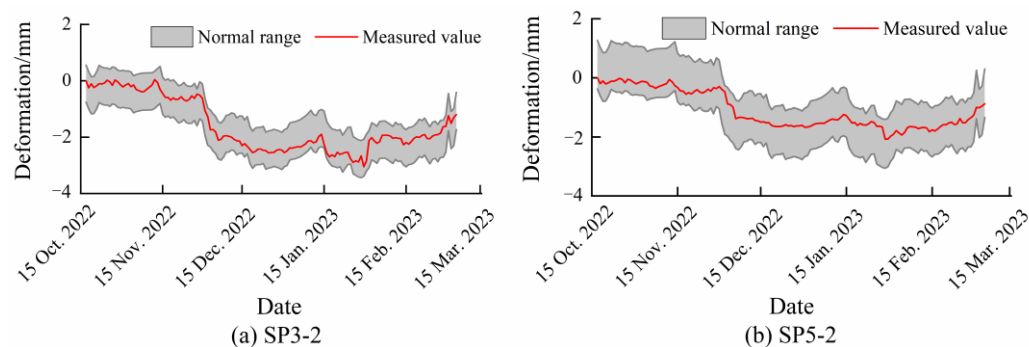


Figure 10. Analysis diagram of deformation behavior for measurement points SP3-2 and SP5-2.

5. Conclusions

Consideration of the sluice structure should focus on the issue of nonuniform deformation due to the uneven property of soft soil foundation. When analyzing the deformation state of a sluice, the traditional methods could not take the nonuniform deformation into account, which is a potential risk in structural safety evaluation. From the perspective of nonuniform deformation, this article proposes a method to determine the deformation behavior of sluice structures. Firstly, we divide the deformation of sluice structures into overall effect and individual effect based on their homogeneity and heterogeneity characteristics, describing the overall deformation trend of the sluice structure and deviation degree between the deformation of single points and the overall deformation separately. Then, in order to explore the influence of hidden factors, panel data theory is introduced to identify the values of overall and individual effects for sluice deformation. Finally, the probability distribution function of individual effect values at each measurement point can be solved based on the maximum entropy principle, and furthermore, the deformation warning indicators for each measurement point can be determined, which provides a novel approach to judging the deformation status of sluice structures.

It should be noted that only the sluice structure is investigated in this study, and future research should consider the potential effects of uneven deformation on other hydraulic structures such as earth dams, embankments, and pump station buildings more carefully.

Author Contributions: Conceptualization, B.L. and Z.M.; Data curation, X.L. (Xiang Luo); Formal analysis, B.L. and Z.M.; Funding acquisition, Z.S. and F.M.; Investigation, D.L.; Methodology, B.L. and Z.M.; Project administration, F.M.; Resources, F.M. and B.L.; Software, W.Y.; Supervision, B.L.; Validation, B.L., Z.M. and Z.S.; Visualization, X.L. (Xing Li); Writing—original draft, B.L. and Z.M.; Writing—review and editing, B.L. and Z.M. All authors have read and agreed to the published version of the manuscript.

Funding: This research was supported by the Modern Multimodal Transportation Laboratory Open Fund Project, grant number MTF2023010, the Yellow River Water Science Research Joint Fund, grant number U2243244, and the National Natural Science Foundation of China, grant number 52179130 and 52209165.

Data Availability Statement: Data is contained within the article.

Conflicts of Interest: The authors declare no conflicts of interest.

References

1. Liang, J.; Li, Z.; Ji, Q.; Lu, W.; Cao, Q.; Ahmed, E. Global Sensitivity Analysis of The Deformation Behavior of Sluice Chamber Structure. *Structures* **2021**, *34*, 4682–4693. [[CrossRef](#)]
2. Gu, Z.; Cao, X.; Liu, G.; Lu, W. Optimizing Operation Rules of Sluices in River Networks Based on Knowledge-driven and Data-driven Mechanism. *Water Resour. Manag.* **2014**, *28*, 3455–3469. [[CrossRef](#)]
3. Peng, J.; Xie, W.; Wu, Y.; Sun, X.; Zhang, C.; Gu, H.; Zhu, M.; Zheng, S. Prediction for the Sluice Deformation Based on SOA-LSTM-Weighted Markov Model. *Water* **2023**, *15*, 3724. [[CrossRef](#)]
4. Zhang, G.; Yu, C.; Guo, G.; Li, L.; Zhao, Y.; Li, H.; Gong, Y. Monitoring Sluice Health in Vibration by Monocular Digital Photography and a Measurement Robot. *KSCE J. Civ. Eng.* **2019**, *23*, 2666–2678. [[CrossRef](#)]

5. Xue, B.; Zhang, S.; Fang, H.; Li, M.; Shi, M. Design Method of Polymer Cut-off Wall Density for Earth Dams Based on Multi-Objective Optimization. *Structures* **2023**, *53*, 199–204. [[CrossRef](#)]
6. Xu, W.; Niu, X.; Zhu, Y. Deformation Behavior and Damage Evaluation of Fly Ash-Slag Based Geopolymer Concrete Under Cyclic Tension. *J. Build. Eng.* **2024**, *86*, 108664. [[CrossRef](#)]
7. Li, F.; Wang, Z.; Liu, G.; Fu, C.; Wang, J. Hydrostatic Seasonal State Model for Monitoring Data Analysis of Concrete Dams. *Struct. Infrastruct. Eng.* **2015**, *11*, 1616–1631. [[CrossRef](#)]
8. Gamse, S.; Oberguggenberger, M. Assessment of Long-term Coordinate Time Series Using Hydrostatic-Season-Time Model for Rock-Fill Embankment Dam. *Struct. Control Health Monit.* **2017**, *24*, e1859. [[CrossRef](#)]
9. Song, J.; Zhang, S.; Chen, Y. Long-term Deformation Safety Evaluation Method of Concrete Dams Based on The Time-Varying Stability of Concrete Material. *Mater. Today Commun.* **2023**, *36*, 106468. [[CrossRef](#)]
10. Salazar, F.; Morán, R.; Toledo, M.; Oñate, E. Data-Based Models for The Prediction of Dam Behaviour: A Review and Some Methodological Considerations. *Arch. Comput. Methods Eng.* **2017**, *24*, 1–21. [[CrossRef](#)]
11. Ma, L.; Ma, F.; Cao, W.; Lou, B.; Luo, X.; Li, Q.; Hao, X. A Multi-Strategy Improved Sooty Tern Optimization Algorithm for Concrete Dam Parameter Inversion. *Water* **2024**, *16*, 119. [[CrossRef](#)]
12. Cao, M.; Qiao, P.; Ren, Q. Improved Hybrid Wavelet Neural Network Methodology for Time-Varying Behavior Prediction of Engineering Structures. *Neural Comput. Appl.* **2009**, *18*, 821–832. [[CrossRef](#)]
13. Mata, J. Interpretation of Concrete Dam Behaviour with Artificial Neural Network and Multiple Linear Regression Models. *Eng. Struct.* **2011**, *33*, 903–910. [[CrossRef](#)]
14. Ranković, V.; Grujović, N.; Divac, D.; Milivojević, N. Development of Support Vector Regression Identification Model for Prediction of Dam Structural Behaviour. *Struct. Saf.* **2014**, *48*, 33–39. [[CrossRef](#)]
15. Wang, S.; Xu, C.; Liu, Y.; Gu, H.; Xu, B.; Hu, K. Spatial Association-Considered Real-time Risk Rate Assessment of High Arch Dams Using Observed Displacement and Combination Prediction Model. *Structures* **2023**, *53*, 1108–1121. [[CrossRef](#)]
16. Lu, T.; Gu, C.; Yuan, D.; Zhang, K.; Shao, C. Deep Learning Model for Displacement Monitoring of Super High Arch Dams Based on Measured Temperature Data. *Measurement* **2023**, *222*, 113579. [[CrossRef](#)]
17. Li, Y.; Bao, T.; Chen, H.; Zhang, K.; Shu, X.; Chen, Z.; Hu, Y. A Large-Scale Sensor Missing Data Imputation Framework for Dams Using Deep Learning and Transfer Learning Strategy. *Measurement* **2021**, *178*, 109377. [[CrossRef](#)]
18. Yang, X.; Yuan, C.; Hou, M.; Zhou, C.; Ju, Y.; Qi, F. Law and Early Warning of Vertical Sluice Cluster Displacements in Soft Coastal Soil. *KSCE J. Civ. Eng.* **2023**, *27*, 698–711. [[CrossRef](#)]
19. Yang, X.; Wang, D.; Xu, Y.; Hou, M.; Wang, Z. Performance Assessment of InSAR-Based Vertical Displacement Monitoring of Sluices in Coastal Soft Soil Area. *KSCE J. Civ. Eng.* **2022**, *26*, 371–380. [[CrossRef](#)]
20. Lou, B.; Ma, F.; Luo, X. Abnormality Diagnosis for Deformation Behavior of Pump Station Buildings Based on Nonlinear Dynamics Model. *J. Hydraul. Eng.* **2023**, *54*, 486–496.
21. Shi, Z.; Gu, C.; Qin, D. Variable-Intercept Panel Model for Deformation Zoning of A Super-High Arch Dam. *SpringerPlus* **2016**, *5*, 898. [[CrossRef](#)] [[PubMed](#)]
22. Shao, C.; Gu, C.; Yang, M.; Xu, Y.; Su, H. A Novel Model of Dam Displacement Based on Panel Data. *Struct. Control Health Monit.* **2018**, *25*, e2037. [[CrossRef](#)]
23. Zhao, E.; Wu, C. Risk Probabilistic Assessment of Ultrahigh Arch Dams Through Regression Panel Modeling on Deformation Behavior. *Struct. Control Health Monit.* **2021**, *28*, e2716. [[CrossRef](#)]
24. Cui, X.; Gu, H.; Gu, C.; Cao, W.; Wang, J. A Novel Imputation Model for Missing Concrete Dam Monitoring Data. *Mathematics* **2023**, *11*, 2178. [[CrossRef](#)]
25. Hu, J.; Ma, F. Zoned Deformation Prediction Model for Super High Arch Dams Using Hierarchical Clustering and Panel Data. *Eng. Comput.* **2020**, *37*, 2999–3021. [[CrossRef](#)]
26. Swamy, P.A. Efficient Inference in a Random Coefficient Regression Model. *Econometrica* **1970**, *38*, 311–323. [[CrossRef](#)]
27. Zellner, A. An Efficient Method of Estimating Seemingly Unrelated Regressions and Tests for Aggregation Bias. *J. Am. Stat. Assoc.* **1962**, *57*, 348–368. [[CrossRef](#)]
28. Jaynes, E.T. On the Rationale of Maximum Entropy Methods. *Proc. IEEE* **1982**, *70*, 939–952. [[CrossRef](#)]
29. Zhang, J.; Gu, C. Maximum Entropy Method for Operational Loads Feedback Using Concrete Dam Displacement. *Entropy* **2015**, *17*, 2958–2972. [[CrossRef](#)]
30. Wu, Z.; Shen, C.; Ruan, H. *Safety Monitoring Theory and Its Application of Hydraulic Structures*, 3rd ed.; Higher Education Press: Beijing, China, 2003.

Disclaimer/Publisher's Note: The statements, opinions and data contained in all publications are solely those of the individual author(s) and contributor(s) and not of MDPI and/or the editor(s). MDPI and/or the editor(s) disclaim responsibility for any injury to people or property resulting from any ideas, methods, instructions or products referred to in the content.